The Journal of Chemical Physics

An efficient time-domain implementation of the multichromophoric Förster resonant energy transfer method

Cite as: J. Chem. Phys. **158**, 064103 (2023); https://doi.org/10.1063/5.0136652
Submitted: 28 November 2022 • Accepted: 17 January 2023 • Accepted Manuscript Online: 18 January 2023 • Published Online: 08 February 2023

Kai Zhong, Hoang Long Nguyen, Thanh Nhut Do, et al.

AIP Publishing

The Journal of Chemical Physics ARTICLE scitation.org/journal/jcp

An efficient time-domain implementation of the multichromophoric Förster resonant energy transfer method

Cite as: J. Chem. Phys. 158, 064103 (2023); doi: 10.1063/5.0136652
Submitted: 28 November 2022 • Accepted: 17 January 2023 •
Published Online: 8 February 2023

Kai Zhong,[1,2] Hoang Long Nguyen,[1,2] Thanh Nhut Do,[2] Howe-Siang Tan,[2] Jasper Knoester,[1,3] and Thomas L. C. Jansen[1,a)]

AFFILIATIONS

[1] Zernike Institute for Advanced Materials, University of Groningen, Nijenborgh 4, 9747 AG Groningen, The Netherlands
[2] School of Chemistry, Chemical Engineering and Biotechnology, Nanyang Technological University, 21 Nanyang Link, Singapore, 637371
[3] Faculty of Science, Leiden University, Einsteinweg 55, 2300 RA Leiden, The Netherlands

[a)] **Author to whom correspondence should be addressed:** t.l.c.jansen@rug.nl

ABSTRACT

The excitation energy transfer (EET) process for photosynthetic antenna complexes consisting of subunits, each comprised of multiple chromophores, remains challenging to describe. The multichromophoric Förster resonance energy transfer theory is a popular method to describe the EET process in such systems. This paper presents a new time-domain method for calculating energy transfer based on the combination of multichromophoric Förster resonance energy transfer theory and the Numerical Integration of the Schrödinger Equation method. After validating the method on simple model systems, we apply it to the Light-Harvesting antenna 2 (LH2) complex, a light harvesting antenna found in purple bacteria. We use a simple model combining the overdamped Brownian oscillators to describe the dynamic disorder originating from the environmental fluctuations and the transition charge from the electrostatic potential coupling model to determine the interactions between chromophores. We demonstrate that with this model, both the calculated spectra and the EET rates between the two rings within the LH2 complex agree well with experimental results. We further find that the transfer between the strongly coupled rings of neighboring LH2 complexes can also be well described with our method. We conclude that our new method accurately describes the EET rate for biologically relevant multichromophoric systems, which are similar to the LH2 complex. Computationally, the new method is very tractable, especially for slow processes. We foresee that the method can be applied to efficiently calculate transfer in artificial systems as well and may pave the way for calculating multidimensional spectra of extensive multichromophoric systems in the future.

I. INTRODUCTION

Electronic excitation energy transfer (EET) is one of the important processes in natural photosynthesis and photochemical conversion.[1–3] In recent decades, much attention has been paid to understanding the mechanism of the EET process in biological systems.

Typically, the photosynthetic light-harvesting apparatus consists of multiple interconnected antenna complexes through which the energy has to flow through several complexes to reach the reaction center, where it is converted to chemical energy. Both the fast energy transfer within individual complexes and the slower inter-complex transfers are crucial for the overall light harvesting process. The EET in the light-harvesting complexes is highly efficient, reaching remarkable quantum efficiencies of 90%, or higher at low-light condition.[4] In other words, almost every absorbed photon reaches the reaction center and forms a charge-separated state. Under high-light conditions, the reaction center is protected by a regulatory mechanism, resulting in the quenching of the excessive excitation energy in the antenna. Neither the molecular details of the latter nor the high efficiency of light harvesting is fully understood. To answer the second question, an accurate method for calculating excitation

energy transfer in large and complex multichromophoric systems is required. The goal of this study is to develop and test a new version of the multichromophoric Förster resonance energy transfer (MC-FRET) method[5,6] by combining it with the Numerical Integration of the Schrödinger Equation (NISE) method[7] to obtain a method that is computationally efficient, especially for slow transfer processes.

Traditionally, the efficiency of EET processes has been treated theoretically using the Förster Resonant Energy Transfer (FRET) theory, which yields a transfer rate between two molecules that is proportional to the overlap between the donor emission spectrum and acceptor absorption spectrum and inversely proportional to the sixth power of the donor–acceptor distance.[8,9] The original theory of Förster only describes the electronic excitation energy transfer from a single chromophoric donor to a single chromophoric acceptor. In the 1990s, the theory was extended in order to describe EET between multichromophoric[5,10,11] subsystems, denoted as the MC-FRET method. This approach overcomes the problem that the transfer pathways often involve multiple coupled donors and/or acceptors. Just like the original FRET method, the MC-FRET method is applicable when the overall transfer process between the donor and the acceptor subsystems is incoherent. Furthermore, this method is valid only when intra-donor and intra-acceptor EET processes are faster than the transfer from the donor to the acceptor complexes. In other words, the MC-FRET method is applicable if the transfer process is dominated by a single rate. Numerous other methods have been developed and applied to describe the EET processes, including the Haken-Strobl-Reineker (HSR) method,[12,13] the NISE approach,[7,14–16] and the Hierarchy of Equations of Motion (HEOM) method.[17–19] In the HSR method, the bath is assumed to be in the white-noise limit, which allows for analytical solutions and, therefore, offers much insight. The NISE method allows using arbitrary bath dynamics. Similar to the HSR method, the effect of the system on the bath is neglected in the NISE method, resulting in relaxation to an infinite-temperature distribution.[20] While the HEOM method is restricted to a harmonic bath, it provides an important golden standard as it is formally exact and describes relaxation to the correct thermodynamic distribution.[17]

In the HSR, NISE, and HEOM methods, the transfer is calculated by explicit time-propagation of the system of interest, and the resulting rate is then extracted, which takes a long time and with low efficiency.[16] On the other hand, the MC-FRET method calculates the overlap of the emission and absorption spectra, which renders MC-FRET to be a very efficient method; it needs fewer computation resources than the others.[16,19] Recently, several variants of the MC-FRET approach, differing in how the donor emission and acceptor absorption spectra are obtained, were compared with others.[16] It was found that the spectra determination step is crucial for the performance of the MC-FRET approach, and in many cases, the NISE method provided better agreement with the HEOM approach than the MC-FRET method. It was not easy, however, to determine whether the failure of the MC-FRET approach was determined by the intrinsic incoherent approximation or failure of the method used to obtain the spectral lineshapes.

This paper presents a new time-domain version of the MC-FRET method derived using perturbation theory on the interaction between the donor and acceptor complexes and the NISE method to describe the subsystems. This makes the new method a rigorous incoherent approximation of the NISE method. In contrast to previous versions of the MC-FRET method,[5,11,21,22] the new version is fully working in the time-domain, providing a computationally efficient method and a quick reality check on the reliability of the obtained EET rate. We first test the new method on small model systems comparable to those previously employed,[11] with focus on strongly coupled ring systems[16] resembling the Light-Harvesting antenna 2 (LH2) of purple bacteria. We then proceed to test the method on the actual LH2 complex. We first construct a simple model to reproduce the experimental absorption spectrum of this system and then use the same parameters to calculate the EET rate from the weakly coupled B800 ring containing nine chromophores to the strongly coupled B850 ring containing 18 chromophores. In addition, we also calculate the EET rate between two B850 rings in two adjacent LH2 complexes. The obtained rates are greatly comparable to the measured rates, which demonstrate the accuracy of our newly developed MC-FRET method.

The study is presented as follows: In Sec. II, we first summarize the formalism of the NISE method and derive the new time-domain MC-FRET method. Subsequently, in Sec. III A, we apply these two methods to a model system containing two weakly coupled dimers. Here, we focus on the general properties and applicability of the method. In Sec. III B, we proceed by testing our new method on systems with a single donor and many acceptors and vice versa. The results for the multiacceptor system are compared with previous benchmark results.[16] The application to the LH2 system is presented in Sec. III C. Finally, in Sec. IV, we summarize our findings and draw conclusions.

II. METHOD

A. Model system

We will use the general framework of Frenkel excitons[23,24] to describe the EET process. For simplicity, we treat all molecules as two-level systems, with a ground state and an optically accessible excited state. We focus on a system with a donor complex consisting of N_D molecules and an acceptor complex of N_A molecules and restrict ourselves to the case of a single excitation shared by all molecules in the system.

The full Hamiltonian for the system is described as follows:

$$H(t) = H_D(t) + H_A(t) + H_{AD}, \tag{1}$$

where $H_D(t)$ and $H_A(t)$ denote the Hamiltonians of the donor and the acceptor complex, respectively, and H_{AD} describes the interaction between them. In the site representation, $H_D(t)$ and $H_A(t)$ are

$$H_D(t) = \sum_n^{N_D} (\epsilon_n^D + \delta\epsilon_n^D(t))|D_n\rangle\langle D_n| + \sum_{n\neq m}^{N_D} J_{nm}^{DD}|D_m\rangle\langle D_n|, \tag{2}$$

$$H_A(t) = \sum_n^{N_A} (\epsilon_n^A + \delta\epsilon_n^A(t))|A_n\rangle\langle A_n| + \sum_{n\neq m}^{N_A} J_{nm}^{AA}|A_m\rangle\langle A_n|, \tag{3}$$

where ϵ_n^D (ϵ_n^A) is the average electronic transition energy of donor molecule n (acceptor molecule n) and $\delta\epsilon_n^D(t)$ ($\delta\epsilon_n^A(t)$) is the time-dependent fluctuation in this energy caused by the interaction with

the (thermal) environment. In this study, we assume that these bath fluctuations for different donor and acceptor molecules are uncorrelated. However, this need not be assumed in general. $|D_n\rangle$ represents the basis state where only the n'th donor molecule is excited while all other donor and acceptor molecules are in their ground state. Similarly, $|A_n\rangle$ is the state with only acceptor molecule n excited. The interaction between different donor (acceptor) molecules is given by J_{nm}^{DD} (J_{nm}^{AA}).

The last term of Eq. (1) represents the coupling between the donor and acceptor complexes and reads

$$H_{AD} = \sum_{m=1}^{N_D}\sum_{n=1}^{N_A} J_{nm}^{AD}(|D_m\rangle\langle A_n| + |A_n\rangle\langle D_m|), \tag{4}$$

where the coupling term J_{nm}^{AD} is the resonance interaction between donor molecule m and acceptor molecule n. These interactions are the ones that ultimately are responsible for the EET process between both complexes. These interactions are time-independent, which is a good approximation in systems with fixed geometry.

The electronic couplings in Eqs. (2), (3), and (4) can, for example, be calculated by the point-dipole approximation,[25] the extended-dipole approximation,[26,27] or the TrEsp method.[28–30] In the TrEsp method, the interaction is given by[28]

$$J_{nm}^{XY} = \frac{1}{4\pi\varepsilon_0\varepsilon_r}\sum_{k=1}^{N_X}\sum_{l=1}^{N_Y}\frac{q_{mk}(1,0)q_{nl}(0,1)}{|\vec{r}_{mk} - \vec{r}_{nl}|}. \tag{5}$$

Here, X and Y represent either A for an acceptor molecule or D for a donor molecule. ε_r is the dielectric constant and $\frac{1}{4\pi\varepsilon_0}$ is the Coulomb constant. $q_{mk}(1,0)$ and $\vec{r}_{mk}$ denote the transition charge and coordinate of one atomic partial charge, respectively. In Section III C, we will apply the TrEsp method to calculate the inter-molecular couplings for the LH2 complex with the transition charges for the bacterial chromophores given in Ref. 28 and the coordinates from the 1kzu protein databank file.[31]

The energy fluctuation term, $\delta\epsilon_m^X(t)$, in Eq. (2) plays a crucial role in the EET process. For simplicity, the Brownian oscillator model is employed to limit the number of free parameters in the description of the dynamic process. We model the bath vibrations as a collection of independent harmonic oscillators, and the excitation energy has a linear dependence on the system-bath coupling.[16] Here, we neglect the influence of the electronic excitation on the bath dynamics. Therefore, the Stokes shift is neglected in the emission. The time correlation function of the dynamic process is fully characterized by

$$C(t) = \left\langle \delta\epsilon_m^X(t)\delta\epsilon_n^Y(0)\right\rangle = \sigma_{Xm}^2\ \exp(-\Lambda|t|)\delta_{XY}\delta_{nm}, \tag{6}$$

where σ_{Xm} denotes the root-mean-squared magnitude of the energy fluctuations for the different donor or acceptor molecules and Λ is the inverse of the correlation time of the bath fluctuations, here to be taken identical for all sites.

The above stochastic dynamic process for the excitation energies is numerically generated in the following way:[32]

$$\delta\epsilon_m^X(t+\Delta t) = \delta\epsilon_m^X(t)\exp(-\Lambda|\Delta t|) + G(\sigma_m^X)\sqrt{1-\exp(-2\Lambda|\Delta t|)}, \tag{7}$$

where $G(\sigma_m^X)$ is a random number taken from a Gaussian distribution with zero mean and standard deviation σ_m^X. Δt is the timestep between frames at which the Hamiltonian is generated. The first term in the equation represents the exponential decay of memory and the second term ensures that the standard deviation in the energy is preserved over the generated trajectory.

B. Methods for calculating the EET rate

1. Numerical integration of the Schrödinger equation (NISE) method

The NISE method[7,14–16] describes the EET process based on the time-dependent Schrödinger equation that describes the exciton wave function,

$$\frac{d\Psi(t)}{dt} = -\frac{i}{\hbar}H(t)\Psi(t). \tag{8}$$

Here, $H(t)$ is the total Hamiltonian in Eq. (1). To solve this equation, we discretize time in short intervals Δt, identical to those used above for the disorder, and treat the Hamiltonian as a constant during the time interval $(t, t+\Delta t)$. This leads to the relation,

$$\Psi(t+\Delta t) = U(t+\Delta t, t)\Psi(t), \tag{9}$$

where $U(t+\Delta t, t)$ is the time evolution matrix,

$$U(t+\Delta t, t) = \exp\left(-\frac{i}{\hbar}H(t)\Delta t\right). \tag{10}$$

The time-evolution for longer times is obtained by multiplying consecutive time-evolution matrices, leading to the expression,

$$U(t,0) = \prod_{j=1}^{t/\Delta t} U(j\Delta t, (j-1)\Delta t). \tag{11}$$

The population transfer between the donor and the acceptor complexes follows from the decay of the total donor population,

$$P_D(t) = \sum_{n=1}^{N_D} |\langle\Psi_D|U(t,0)|\Psi_D\rangle|^2. \tag{12}$$

Here, Ψ_D same as $|D_n\rangle$. To obtain the transfer rate, the result for $P_D(t)$ is fitted to an exponentially evolving function, having the form as

$$f(t) = P_D^{eq} + c(1 - P_D^{eq})e^{-k_{eff}t}. \tag{13}$$

Here, k_{eff} is the effective rate that can be obtained through the NISE method directly. The EET rate from the donor complex to the acceptor complex, k can be calculated with k_{eff},

$$k = (1 - P_D^{eq})k_{eff}, \tag{14}$$

where P_D^{eq} is the donor excitation probability in the equilibrium state. The parameter c is introduced to account for a possible initial part of the decay that is affected by transient coherences; if such coherences occur, the corresponding initial dynamics of P_D is discarded from the fitting procedure. Furthermore, c also indicates

whether the excitation population decays exponentially or not. For fully incoherent transfer, $c = 1$, where the excitation population is exponentially decaying. The closer c is to 1, the more incoherent it is.

The main advantages of the NISE method are that it does not rely on a perturbative treatment of the donor–acceptor interactions and that it can be used to analyze the EET process accounting for coherent and incoherent effects equally well. The most notable disadvantages of the NISE method are its intrinsic high-temperature character, resulting in an equilibrium state of equal probability for all exciton states, and the neglect of the Stokes shift as a result of the omission of the imaginary part of the bath correlation function. Furthermore, to obtain accurate results, we need to average over the bath fluctuations, which require averaging over numerous independent trajectories. Especially, in the case of weak donor–acceptor interactions in an extensive system ($N_D, N_A \gg 1$), the computation is expensive because the population needs to be calculated for long time delays to get accurate rates and determining the matrix exponent in Eq. (10) is an order $(N_A + N_D)^3$ process.

2. Multichromophoric Förster resonant energy transfer (MC-FRET) method

The MC-FRET method[5,10,11] is a well-known approach to calculating the transfer rate for a multichromophoric system. It describes the incoherent EET process that occurs after the donor complex has been excited to a singly excited state. In the following, we present a new derivation of the MC-FRET method as a perturbative approximation to the NISE method described in Sec. II B 1. The probability that the acceptor complex is excited at time t if it is in the state $|\Psi(0)\rangle$ at time zero is

$$P_A(t) = \sum_{n=1}^{N_A} \langle\langle A_n|U(t,0)|\Psi(0)\rangle\langle\Psi(0)|U(0,t)|A_n\rangle\rangle = \sum_{n=1}^{N_A} \langle\langle A_n|U(t,0)\rho(0)U(0,t)|A_n\rangle\rangle, \quad (15)$$

where $\langle\ldots\rangle$ denotes the ensemble average, i.e., the average over the bath fluctuations, $U(t,0)$ is the time-evolution operator, and $\rho(0) = |\Psi(0)\rangle\langle\Psi(0)|$ is the density operator of the initial state.

Next, we apply first-order time-dependent perturbation theory in the interaction between the donor and acceptor complexes, H_{AD}. In this derivation, we may even assume that these interactions are time-dependent. We then obtain

$$\begin{aligned} P_A(t) &= \sum_{n=1}^{N_A} \Big\langle\Big\langle A_n|U_0(t,0)\Big(1 - \frac{i}{\hbar}\int_0^t U_0(0,\tau_1)H_{AD}(\tau_1)U_0(\tau_1,0) \\ &\quad \times d\tau_1\Big)\rho(0)\Big(1 + \frac{i}{\hbar}\int_0^t U_0(0,\tau_2)H_{AD}(\tau_2)U_0(\tau_2,0)d\tau_2\Big) \\ &\quad \times U_0(0,t)|A_n\rangle\Big\rangle \\ &= \frac{1}{\hbar^2}\sum_{n=1}^{N_A} \Big\langle\Big\langle A_n|U_0(t,0)\int_0^t U_0(0,\tau_1)H_{AD}(\tau_1)U_0(\tau_1,0)d\tau_1 \\ &\quad \times \rho(0)\int_0^t U_0(0,\tau_2)H_{AD}(\tau_2)U_0(\tau_2,0)d\tau_2\Big)U_0(0,t)|A_n\Big\rangle\Big\rangle. \end{aligned} \quad (16)$$

Here, $U(t,0)$ is the time-evolution operator corresponding to the full Hamiltonian [Eq. (1)], while $U_0(t,0)$ is the time-evolution operator excluding the perturbative term describing the interaction between the donor and acceptor complexes. The second step in Eq. (16) can be made because in the initial state $\rho(0)$ only molecules in the donor complex are excited. Next, we substitute Eq. (4) for H_{AD} to obtain,

$$P_A(t) = \frac{1}{\hbar^2}\sum_{a,c=1}^{N_D}\sum_{b,d=1}^{N_A}\int_0^t\int_0^t d\tau_1 d\tau_2 \big\langle J_{ba}^{AD}(\tau_1)J_{cd}^{DA}(\tau_2)\big\rangle \times \langle A_d|U_0(\tau_2,\tau_1)|A_b\rangle\langle D_a|U_0(\tau_1,0)\rho(0)U_0(0,\tau_2)|D_c\rangle\rangle, \quad (17)$$

where we generalized to time-dependent donor–acceptor interactions $J_{mn}^{AD}(t)$.

To obtain the donor–acceptor EET rate, we now nest the integral over τ_2 inside the one over τ_1 and split the first one into integrals from 0 to τ_1 and from τ_1 to t. By interchanging in the second contribution the dummy integration variables (τ_1 and τ_2) and the dummy summation variables (a and c; b and d), the two terms arising from this splitting may be shown to be each other's complex conjugates, which leads to

$$P_A(t) = \frac{2\mathrm{Re}}{\hbar^2}\sum_{a,c=1}^{N_D}\sum_{b,d=1}^{N_A}\int_0^t\int_0^{\tau_1} d\tau_1 d\tau_2 \big\langle J_{ba}^{AD}(\tau_1)J_{cd}^{DA}(\tau_2)\big\rangle \times \langle A_d|U_0(\tau_2,\tau_1)|A_b\rangle\langle D_a|U_0(\tau_1,0)\rho(0)U_0(0,\tau_2)|D_c\rangle\rangle. \quad (18)$$

By taking the derivative of this expression with respect to t, one obtains a time-dependent EET rate in the form,

$$k(t) = \frac{2\mathrm{Re}}{\hbar^2}\sum_{a,c=1}^{N_D}\sum_{b,d=1}^{N_A}\int_0^t d\tau_2 \big\langle J_{ba}^{AD}(t)J_{cd}^{DA}(\tau_2)\big\rangle\langle A_d|U_0(\tau_2,t)|A_b\rangle \times \langle D_a|U_0(t,0)\rho(0)U_0(0,\tau_2)|D_c\rangle\rangle. \quad (19)$$

In this equation, we may rewrite $U_0(t,0)\rho(0)U_0(0,\tau_2) = U_0(t,\tau_2)U_0(\tau_2,0)\rho(0)U_0(0,\tau_2) = U_0(t,\tau_2)\rho_e^D$, with $\rho_e^D = \frac{e^{-\beta H_0^D}}{\mathrm{Tr}e^{-\beta H_0^D}}$ the equilibrium density operator of the donor complex (H_0^D is the initial Hamiltonian for the donor complex, $\beta^{-1} = k_B T$ with k_B the Boltzmann's constant and T the temperature). In the last step, we have assumed that equilibration within the donor complex is fast compared with the EET time between the donor and the acceptor complexes. This is an assumption that underlies the MC-FRET method anyhow, as it presumes that a single rate can describe the EET process. Now changing to the new integration variable $\tau = \tau_2 - t$ and using the stationary nature of the dynamic disorder, we arrive at

$$k(t) = \frac{2\mathrm{Re}}{\hbar^2}\sum_{a,c=1}^{N_D}\sum_{b,d=1}^{N_A}\int_{-t}^0 d\tau \big\langle J_{ba}^{AD}(0)J_{cd}^{DA}(\tau)\big\rangle\langle A_d|U_0(\tau,0)|A_b\rangle \times \big\langle D_a|U_0(0,\tau)\rho_e^D|D_c\big\rangle\big\rangle. \quad (20)$$

We now take the limit $t \to \infty$ and replace the integration variable τ by t again. Finally, we use the fact that the real part of the integrand is an even function of time, to obtain the EET rate,

$$k = \frac{2\mathrm{Re}}{\hbar^2}\sum_{a,c=1}^{N_D}\sum_{b,d=1}^{N_A}\int_0^\infty dt \times \left\langle J_{ba}^{AD}(0)J_{cd}^{DA}(t)\langle A_d|U_0(t,0)|A_b\rangle\left\langle D_a|U_0(0,t)\rho_e^D|D_c\right\rangle\right\rangle. \quad (21)$$

Equation (21) is the most general expression for the EET rate between the donor and the acceptor complex within the MC-FRET method. If we now assume, as we will do in all applications below, that the donor–acceptor interactions are time-independent and that we may neglect correlations between the bath fluctuations on the donor and the acceptor molecules, we arrive at

$$k = \frac{2\mathrm{Re}}{\hbar^2}\int_0^\infty dt\ \mathrm{Tr}[J^{AD}E^D(t)J^{DA}I^A(t)], \quad (22)$$

with $I^A(t)$ and $E^D(t)$ matrices with their elements defined by

$$I_{db}^A(t) = \langle\langle A_d|U_0(t,0)|A_b\rangle\rangle, \quad (23)$$

and

$$E_{ac}^D(t) = \left\langle\left\langle D_a|U_0(0,t)\rho_e^D|D_c\right\rangle\right\rangle, \quad (24)$$

where J^{AD} is the $N_A \times N_D$ matrix with elements J_{ba}^{AD} and J^{DA} its Hermitian conjugate. From here onwards, we will denote $\mathrm{Re}[\mathrm{Tr}[J^{AD}E^D(t)J^{DA}I^A(t)]]$ as the transfer response.

We will find this transfer response to be useful in evaluating whether the incoherent approximation holds. The MC-FRET theory differs from the original Förster's (FRET) theory[8,9,33] describing EET from a single donor to a single acceptor molecule, in the fact that $I^A(t)$ and $E^D(t)$ are matrices. Furthermore, the interaction term J in conventional FRET theory[8,9,33] is calculated using the dipole–dipole approximation.[34,35] Here, we will use fixed numbers or apply the TrEsp method to obtain the inter-molecular coupling.

In the present MC-FRET formulation, we calculate the emission and absorption response, $E_{ac}^D(t)$ and $I_{db}^A(t)$, in the time domain instead of calculating the overlap of the emission spectrum and the absorption spectrum as was done in previous MC-FRET work.[5,11] Therefore, we will name the new version of the MC-FRET method as TD-MC-FRET. These responses are calculated using the NISE[7,14,15] method, which is straightforward when compared with other approximations.[6,36–38] This also results in the present formulation of TD-MC-FRET being a rigorous approximation to the NISE approach applicable in the incoherent limit. Therefore, when the assumptions are valid that (i) the transfer between the donor and acceptor complexes is incoherent and (ii) the transfer within the donor/acceptor complexes is faster than that from the donor to the acceptor complex, the two methods should give identical results. We note that should the couplings between donor and acceptor complexes be time-dependent or if the fluctuations in both complexes are correlated, the expression can be replaced by one where the ensemble averages are removed from the individual matrices and taken over the full trace.

Both the NISE and the MC-FRET methods will lead to the high-temperature equilibrium between the units involved. A few thermalizations approaches have been proposed for the NISE method[39–41] and for MC-FRET, for example, the Oxtoby quantum correction[42] can be applied. The quantum correction of Oxtoby only changes the equilibrium populations, but not the time-scale of the transfer defined by the sum of the forward and backward rates. In the present study, we will stick to the high-temperature thermalization approximation to avoid deviating from the main focus of the paper.

III. RESULTS

In this study, we employed the NISE and TD-MC-FRET methods to calculate the EET rate between the B850 and B800 rings of the LH2 system as well as the transfer rate between two B850 rings of two neighboring LH2 units. The LH2 system of purple bacteria consists of two rings of bacteriochlorophyll molecules with the B850 ring being narrower than the B800 ring.[43–45] The B850 pigments are close to each other, separated by ~9 Å while the distance between the B800–B800 and B800–B850 pigments is ~18 Å.[46–48] Therefore, the exciton states in the B850 ring tend to be quite delocalized, while those in the B800 ring are largely localized.

A. Test for different dynamic disorder magnitudes

To test our new TD-MC-FRET method, we first applied the TD-MC-FRET and NISE methods to a simple model system containing two donor and two acceptor molecules. All molecules interact with each other. They also interact with the bath, which leads to transition energy fluctuations, modeled as described in Sec. II A. We employed two different disorder values, $\sigma = 200$ and 45 cm^{-1}, which resemble the more localized B800 ring and the more delocalized B850 ring, respectively. In both cases, $\Lambda = \frac{1}{150}$ fs^{-1} was used. The Hamiltonian of the model system is inspired by Ref. 11, which uses the angular wavenumbers; specifically, we use

$$H_s^D = \begin{pmatrix} 200 & 100 \\ 100 & 180 \end{pmatrix}, \quad H_s^A = \begin{pmatrix} 100 & 100 \\ 100 & 80 \end{pmatrix}. \quad (25)$$

The couplings between the donor complex and the acceptor complex govern the EET rate. For simplicity, we consider all the couplings between the donor and acceptor molecules to be identical, $J = 5$ cm^{-1}, for $m, n \in \{1, 2\}$. The effects of the inter-complex coupling J on the EET rate with dynamic disorder $\sigma = 200$ cm^{-1} are shown in Fig. 1. For each choice of J, we ran five independent simulations for each simulation and averaged over 3000 random realizations of the Hamiltonian trajectories to obtain accurate results. Based on the variations between the five simulations, the results have an error bar less than 3% for the NISE method and smaller than 1% for the TD-MC-FRET method. As discussed in Sec. II, the initial condition is assumed to be a single excitation incoherently distributed over all donor molecules with equal weights, i.e., $\rho(0) = \frac{\mathbb{1}}{2}$ is employed in the TD-MC-FRET method. In the NISE method, this initial condition is realized by averaging the results obtained starting from the totally symmetric and totally antisymmetric initial conditions, respectively.

As can be seen in Eq. (22), in the TD-MC-FRET method, the EET rate is proportional to J^2. Hence, the EET rate for all other couplings can straightforwardly be calculated based on the EET rate

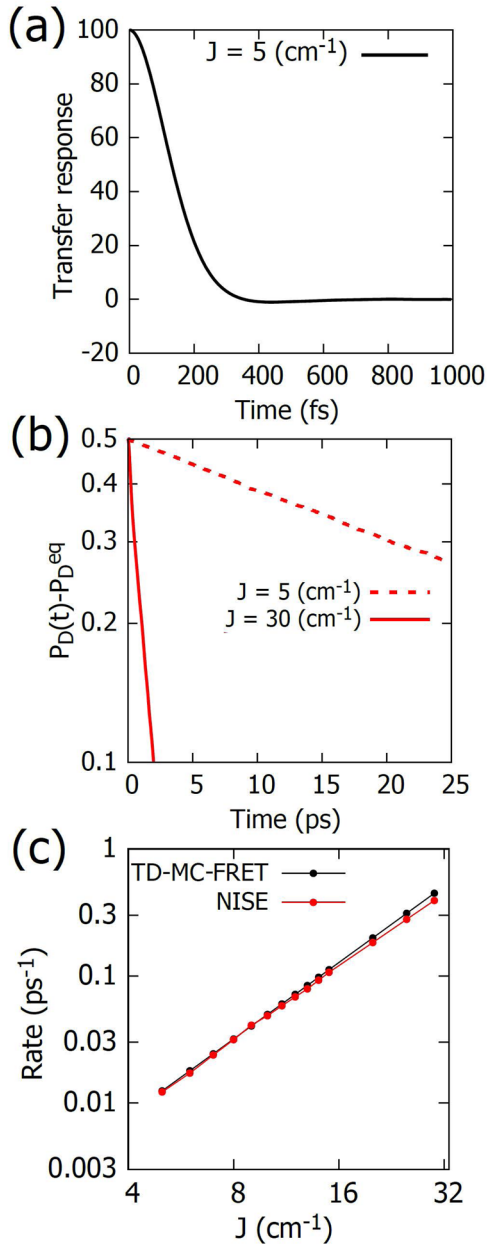

FIG. 1. Comparison of the EET rate between two coupled dimers, described by the Hamiltonian in Eq. (25) as a function of the donor–acceptor coupling J for the NISE method and the TD-MC-FRET method with dynamic disorder $\sigma = 200$ cm^{-1}. (a) The transfer response for the TD-MC-FRET method obtained for the coupling $J = 5$ cm^{-1}. (b) Semi-logarithmic plot of the donor population relaxation calculated with the NISE method for $J = 5$ and 30 cm^{-1}. (c) Double-logarithmic plot of the resulting EET rates with the coupling J varied from 5 to 30 cm^{-1}.

for $J = 5$ cm^{-1}. Figure 1(a) shows the transfer response defined below Eq. (24) for $J = 5$, from which the EET rate for the TD-MC-FRET method is calculated by integrating it over time. The transfer response relaxes to zero; fitting the decay to an exponential function gives a decay rate of 8.7 ps^{-1}, which reflects the loss of coherence between the donor and acceptor dimers at a timescale of about 115 fs. For the NISE method, the EET rate was obtained by analyzing the population dynamics. Figure 1(b) shows a semi-logarithmic plot of the time dependence of the total donor population relative to its equilibrium value using the NISE method for $J = 5$ cm^{-1} (red dash line) and 30 cm^{-1}(red solid line). The two straight lines clearly demonstrate the exponential nature of the population relaxation, suggesting that the transfer between the donor and acceptor complexes is incoherent. Here, we need to mention the results in Figs. 1(a) and 1(b) [also in Figs. 2(a) and 2(b) below] are plotted for just one of the five simulation samples, as those obtained from all other samples fall on top of each other. The slope of the lines in Fig. 1(b) is k_{eff} [Eq. (13)] from which the donor–acceptor EET rate k is obtained by using Eq. (14). For $J = 30$ cm^{-1} the population relaxes to the equilibrium state within 5 ps. For $J = 5$ cm^{-1}, on the other hand, the system even does not reach equilibrium in a 50 ps simulation. Obviously, to get an accurate EET rate using the NISE method, trajectories are needed that are longer than the relaxation time. This is in stark contrast to the TD-MC-FRET method, where the transfer response relaxes within 400 fs, so we do not need to simulate the full transfer process to obtain the rate. Figure 1 directly demonstrates that the time needed to calculate the EET rate using the NISE method strongly depends on the strength of coupling and illustrates the computational efficiency of the TD-MC-FRET method.

Finally, Fig. 1(c) shows J dependence of the EET rate for the model system calculated with the NISE and TD-MC-FRET methods for dynamic disorder strength $\sigma = 200$ cm^{-1}. It shows that the EET rates are identical for both methods, even when increasing the coupling. This is because, in our TD-MC-FRET implementation, the emission response and the absorption response are calculated using the NISE method, which for the current system parameters leads to almost the same transfer rate for both methods. Only for the largest values of the donor–acceptor interactions, do we observe a small deviation between both methods, which results from the fact that, unlike NISE, the TD-MC-FRET method relies on a perturbation expansion in this interaction. This, thus, demonstrates the accuracy and correct implementation of our developed TD-MC-FRET method to describe EET processes in the perturbative limit. Furthermore, in Fig. 1(c), the average over all the samples for different couplings to obtain the parameter c [in Eq. (13)] is 0.985, which is very close to 1 reflecting the incoherent nature of the EET process.

Next, we focus on the case of small dynamic disorder ($\sigma = 45$ cm^{-1}). Figure 2(a) shows that the transfer response looks very different from the case of large dynamic disorder. It shows a damped oscillation, with a damping rate of 0.42 ps^{-1} (obtained from fitting a cosine function multiplied by an exponential function). In Fig. 2(b), the NISE method is seen to predict a transfer time of the order of 150 ps for $J = 5$ cm^{-1}, which is much slower than in Fig. 1(b). The average over five independent samples to obtain the value of the parameter c for the results shown in Fig. 2(c) is 1.003, which suggests that the transfer is incoherent and the excitation population decays almost perfectly exponentially. Figure 2(c) shows the dependence of the EET transfer rate on the donor–acceptor coupling for both methods. This figure clearly demonstrates the breakdown of the perturbation theory underlying the TD-MC-FRET method for growing

coupling. The reason that the discrepancy between both methods appears at a much smaller coupling than in Fig. 1(c) is that the small parameter in Förster's perturbation theory is the ratio of J and the optical dephasing rate. The latter is much smaller for dynamic disorder $\sigma = 45\ \mathrm{cm}^{-1}$, i.e., the decoherence time between donor and acceptor is much smaller.

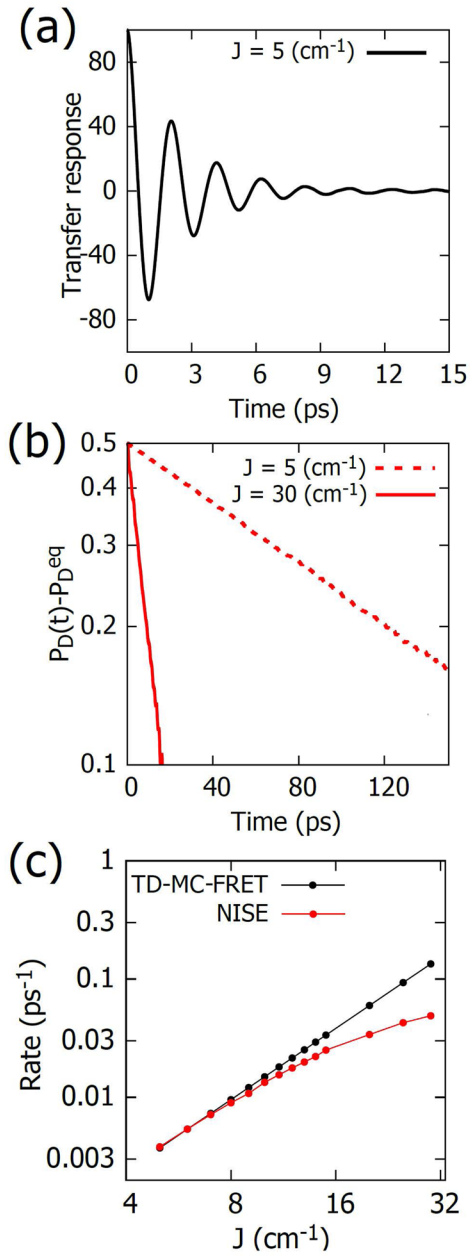

FIG. 2. Comparison of the EET rate between two coupled dimers, described by the Hamiltonian in Eq. (25) as a function of the donor–acceptor coupling J for the NISE method and the TD-MC-FRET method with small dynamic disorder $\sigma = 45\ \mathrm{cm}^{-1}$. (a) The transfer response for the TD-MC-FRET method calculated for the coupling $J = 5\ \mathrm{cm}^{-1}$. (b) Semi-logarithmic plot of the population relaxation calculated with the NISE method at coupling $J = 5$ and $30\ \mathrm{cm}^{-1}$. (c) Double-logarithmic plot of the resulting EET rates with the coupling J varied from 5 to $30\ \mathrm{cm}^{-1}$.

In fact, the combination of Figs. 2(a) and 2(c) demonstrates that if the transfer rate predicted by the TD-MC-FRET becomes large than roughly one-tenth of the transfer response rate, the TD-MC-FRET method starts to break down. The exact value may be system dependent, but intuitively it makes sense that if the transfer rate and the transfer response rate become comparable in magnitude, the TD-MC-FRET theory breaks down. Comparing the decay of the transfer response with the predicted transfer time thus provides an internal consistency check for the TD-MC-FRET method. Thus, we can evaluate the validity without explicitly performing the full NISE transfer rate calculation.

B. Multidonor and multiacceptor systems

To further test our new method, we next studied two model systems that are more similar to the real LH2 system. The first has a monomeric donor molecule, while the acceptor complex is a ring consisting of N_A molecules, with N_A ranging from 1 to 10 [see Fig. 3(a)]. The second model has the opposite configuration, with one acceptor molecule, while the donor complex is a ring with a varying number of molecules, N_D, ranging from 1 to 10 [see Fig. 4(a)]. We assumed that in both system, all the molecules have a transition dipole moment in the same direction, perpendicular to the plane of the ring, and for simplicity, we restricted ourselves to nearest-neighbor excitation transfer interactions J_{DD} and J_{AA} within the donor and acceptor complexes, respectively. We averaged over five independent samples with different white noises; each sample averaged over 1000 random realizations of the Hamiltonian trajectories to obtain the EET rate both for the TD-MC-FRET and NISE methods. The initial condition for the NISE method is an incoherent distribution of the donor complex.

We tested different choices for the initial condition and found that for all used parameters the results were essentially identical with situations where we used a fully local or a fully coherent delocalized initial condition. In cases, where the relaxation within the donor is much slower or comparable to the transfer time to the acceptor, one may find that the choice of initial state will be important.

The initial density matrix of the donor complex for the TD-MC-FRET method was constructed to have equal weight for all populations and all coherences were set to zero in the site basis.

The Brownian oscillator model was applied to generate the dynamic disorder with a correlation time of 150 fs for all the systems. The intra-complex couplings were set to $J_{DD} = J_{AA} = 300\ \mathrm{cm}^{-1}$, while the donor–acceptor coupling was taken $J_{AD} = 20\ \mathrm{cm}^{-1}$ for all pairs of molecules.[16] We choose these parameters to mimic realistic parameters based on the real LH2 system.[30,49] To compare with the reference data, Ref. 16, we also use the angular wavenumbers for the calculation.

Figures 3(b) and 3(c) show the results for the EET rate for the first model system as a function of N_A. The EET rate was calculated using the NISE method and the TD-MC-FRET method with two different dynamic disorder magnitudes, namely $\sigma = 1000\ \mathrm{cm}^{-1}$ [panel (b)] and $200\ \mathrm{cm}^{-1}$ [panel (c)]. For comparison, we also plot the results using three other methods,[16] two alternative types of MC-FRET rates, labeled with $\mathrm{MC-FRET}^{\mathrm{diag}}$ and $\mathrm{MC-FRET}^{\mathrm{diag},IPR}$, and the HEOM rate. The $\mathrm{MC-FRET}^{\mathrm{diag}}$ method uses the diagonal (secular) MC-FRET approximation[37,38,50] and is also referred to as

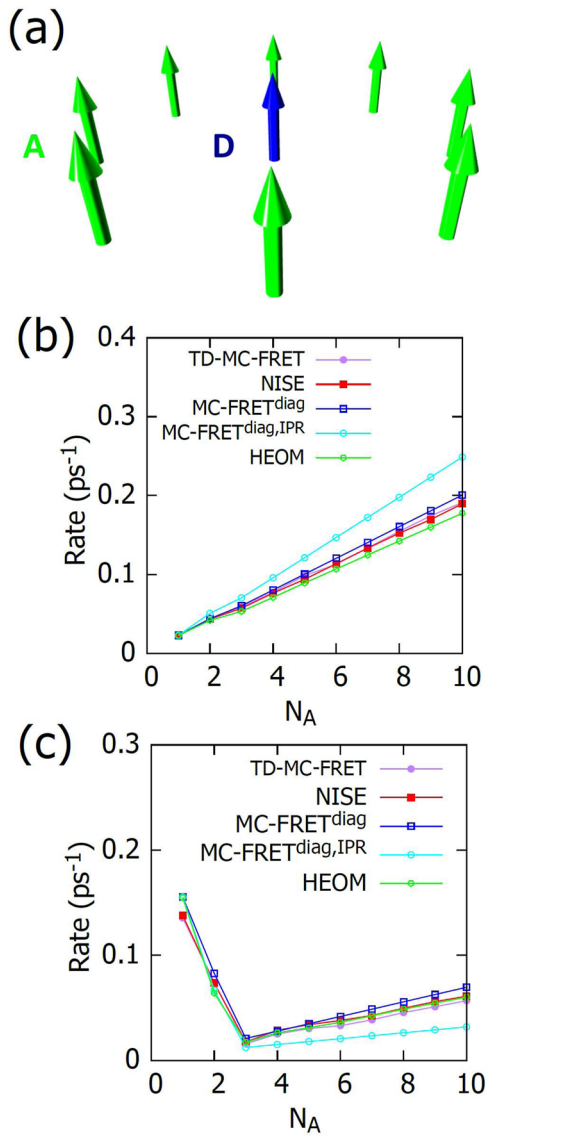

FIG. 3. (a) Illustration of a single donor surrounded by a ring of N_A acceptor molecules. The donor molecule (blue) is placed in the center of the ring and is coupled to each of the acceptor molecules (green) with an interaction $J_{AD} = 20\ \text{cm}^{-1}$. Neighboring acceptor molecules have a coupling $J_{AA} = 300\ \text{cm}^{-1}$, while long–range interactions are set to zero. (b) Transfer rate from the donor molecule to the acceptor ring, using the two main methods (NISE and TD-MC-FRET) introduced in this work, compared with the results from three other methods reported in Ref. 16 (see text). The dynamic disorder was chosen $\sigma = 1000\ \text{cm}^{-1}$ (c) As (b), but now using $\sigma = 200\ \text{cm}^{-1}$.

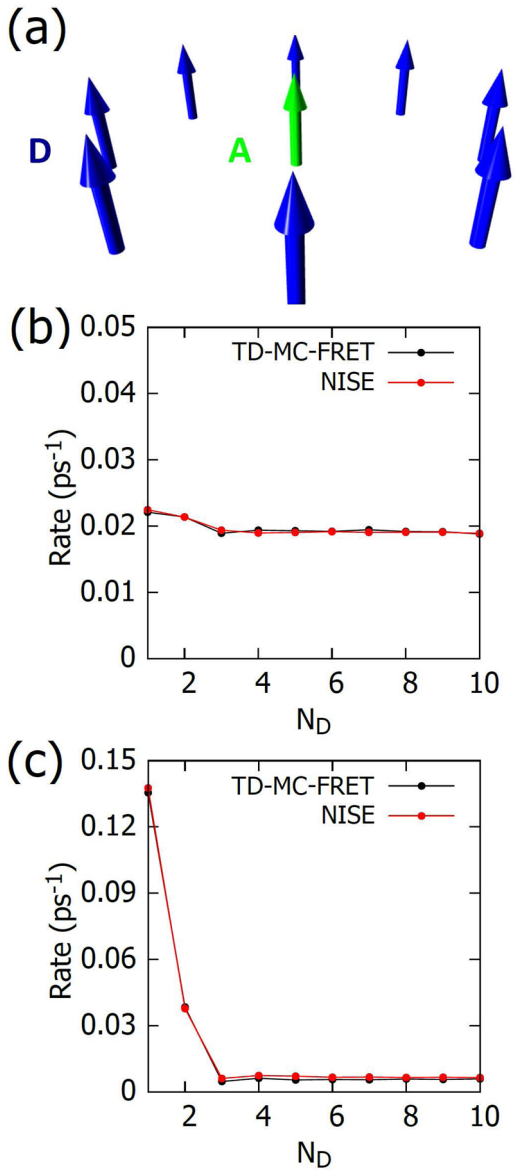

FIG. 4. (a) Illustration of a single acceptor surrounded by a ring of N_A donor molecules. The acceptor molecule (green) is placed in the center of the ring and is coupled to each of the donor molecules (blue) with an interaction $J_{AD} = 20\ \text{cm}^{-1}$. Neighboring acceptor molecules have a coupling $J_{DD} = 300\ \text{cm}^{-1}$, while long–range interaction are set to zero. (b) Transfer rate from the donor ring to the acceptor molecule, using the two main methods (NISE and TD-MC-FRET) introduced in this work. The dynamic disorder was chosen $\sigma = 1000\ \text{cm}^{-1}$, and the initial condition was set to an incoherent superposition of one excitation quantum on all donor molecules with equal weight. (c) As (b), but now using $\sigma = 200\ \text{cm}^{-1}$.

the generalized Förster rate. It assumes that the acceptor absorption density operators are diagonal on the eigenstate basis. The MC – FRET$^{\text{diag},IPR}$ is based on the MC – FRET$^{\text{diag}}$ method but takes into account the exchange narrowing of the absorption spectrum of the acceptor complex through the inverse participation ratio (IPR).[51]

The Hierarchy of Equations of Motion (HEOM) method is based on the exact equations of motion for a system with bilinear coupling to a quantum-mechanical harmonic oscillator bath.[16,17,52,53]

The results in Fig. 3(b) show that the EET rate increases linearly with the number of acceptor molecules. This can be understood

from the fact that the coupling between the acceptors of 300 cm^{-1} is much smaller than the dynamic disorder. The number of acceptor molecules, therefore, does not significantly affect the absorption line shape of the acceptor ring and, therefore, the overlap between the acceptor absorption and donor emission responses hardly depends on N_A. The transfer rate then essentially scales proportionally to the number of independent acceptors that the excitation can transfer to. We note that the TD-MC-FRET results (purple) and the NISE results (red) overlap almost perfectly, making it hard to distinguish them. Both methods are close to the exact HEOM results (deviation of a few percent). Of the two other MC-FRET methods, MC – $FRET^{diag}$ deviates roughly a factor of two more, while MC – $FRET^{diag,IPR}$ deviates significantly.

Figure 3(c) demonstrates that for small disorder ($\sigma < J_{AA}$), the dependence on N_A is more complicated. In this case, the maximum transfer rate occurs for $N_A = 1$. It drops when increasing to $N_A = 3$ before it increases linearly for N_A beyond 4. This non-monotonic behavior can be explained as follows: The monomer energy of donor and acceptor molecules is identical, which, given the fact that there is no Stokes shift results in a maximal spectral overlap. For the dimeric acceptor system with $\sigma \ll J_{AA}$, the overlap between the absorption and emission spectra decreases, because the acceptor spectrum splits and the accepting state lies higher in energy than the emission of the donor excited state. Furthermore, because of the exchange narrowing in the acceptor complex, the linewidth of the absorption spectrum changes significantly for $N_A = 2, 3$. The combination of the above results in a lowering of the overlap between the donor emission and acceptor absorption spectra when increasing N_A from 1 to 3, which explains the decreasing trend in the rate. When we increase the number of acceptor molecules further, the energy of the excitonic acceptor state that overlaps with the donor state and the spectral linewidth hardly change anymore. The transfer rate then only depends on the number of accessible acceptor molecules. All methods giving the EET rate show the same nonmonotonic behavior, yet they also show deviations from each other. The TD-MC-FRET and the NISE methods show almost identical results both very close to the golden standard set nu the HEOM method. The MC – $FRET^{diag}$ method overestimates the HEOM rate while the MC – $FRET^{diag,IPR}$ underestimates it, especially for a large number of acceptor molecules. The latter behavior was also explained in Ref. 16.

Figure 4 shows the results with a ring of N_D donor molecules surrounding one acceptor molecule. Figure 4(a) illustrates the model system; the parameters are the same as for the multiacceptor model system described above. Figure 4(b) shows the transfer rate as a function of N_D with the dynamic disorder set to $\sigma = 1000$ cm^{-1}.The rate is seen to be maximal for $N_D = 1$. It slightly decreases when increasing the ring size to $N_D = 3$ and then stays approximately constant when further increasing N_D. We can understand these results as follows: Similar to the case of Fig. 3(b), the dynamic disorder is significantly larger than the coupling within the donor complex, resulting in small changes of the overlap integrals with varying N_D. In particular, the emission spectrum is almost constant when N_D rises above four. Above this number of donor molecules, the rate is essentially constant as initially, the donors share one excitation quantum and any donor molecule has just one acceptor molecule to transfer its excitation to, independent of the overall number of donors.

For the case of small dynamic disorder [see Fig. 4(c)], the transfer rate has a similar trend as for the case of 1000 cm^{-1} dynamic disorder. However, now the transfer rate decreases significantly when we increase the number of donors from one to three before it becomes constant when the N_D rises above three. The strong decrease in the rate from $N_D = 1$ to 3 finds, like in Fig. 3(c), its origin in the energy shift of the exciton state when increasing the system size, which has a pronounced effect on the spectral overlap for small dynamic disorder.

The situations in Figs. 3 and 4 are actually related by the simple relationship, $\frac{k_{x\to y}}{k_{y\to x}} = \frac{N_y}{N_x}$, directed by the fact that in equilibrium all states are equally likely to be populated. Both Figs. 3 and 4 show that the transfer rates calculated with the TD-MC-FRET method and the NISE method are very close. The excellent agreement demonstrates that our new method can, as expected, accurately describe the EET process for these systems.

C. LH2 system

Finally, we move to the LH2 system. For purple bacteria, this system consists of two rings of bacteriochlorophyll molecules, as described before.[43–45] Based on the absorption wavelength of the two resulting bands, the two rings are denoted the B850 and B800 rings.[30,43,54] The high-frequency ring contains 8–12 bacteriochlorophyll molecules depending on the bacterial species, leading to the B800 band. The low-frequency ring contains twice as many bacteriochlorophyll molecules as the high-frequency ring, and its absorption is red-shifted to 850 nm, resulting in the B850 absorption band. We focus on the *Rhodoblastus acidophilus* (with the old name *Rhodopseudomonas acidophila*) bacterial system depicted in Fig. 5, which contains 27 bacteriochlorophylls (9 B800 bacteriochlorophyll molecules and 18 B850 bacteriochlorophyll molecules).[55]

We employ the simplest Frenkel exciton Hamiltonian for the LH2 system. The general form of the Hamiltonian is shown in Eqs. (2) and (3). We begin with the crystal structure taken from the 1 kzu protein data bank file.[31] The three-fold symmetry specified in the data file was used to construct the full 27 chromophore system. The B850 chromophores were given an average transition frequency of 11 955 cm^{-1}, whereas a 12 465 cm^{-1} transition frequency was

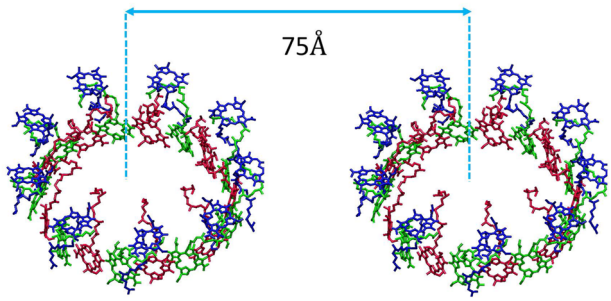

FIG. 5. Schematic overview of two B800–B850 LH2 complexes of *R. acidophilus*. In each complex, the bacteriochlorophylls form two concentric rings of bacteriochlorophyll molecules. The B850 densely packed ring contains two different types of binding pockets, which are α-B850 (green) and β-B850 (red). The other ring only has binding pockets γ-B800 (blue). The center-to-center distance of the two LH2 complexes is 75 Å.[56] The picture was rendered using VMD.[57]

given to the B800 chromophores. Both chromophore types were coupled to an overdamped Brownian oscillator bath with a 150 fs correlation time and disorder magnitudes σ = 256 and 169 cm^{-1} for the B850 and B800 chromophores, respectively. The timestep was set to 3 fs, and the length of the trajectories was taken 30 ps. These numbers were obtained starting with disorder values from literature[43] and scaling of the dynamic disorder for the B850 band with 0.8 and 1.2 for the B800 band to match the experimental absorption spectrum and the EET rate. Here, we need to note that to compare with the experimental results, we use the spectroscopic wavenumbers for the calculation.

The excitonic couplings were determined using the TrEsp model [see Eq. (5)] with the transition charges calculated by the TDDFT/B3LYP method.[28–30] Polarization effects on the couplings between pigments were included via the dielectric constant, ε_r, which is system-dependent. Here, we chose the rescaling factor caused by the dielectric constant, $1/\varepsilon_r$ = 0.55, to match both the experimental absorption spectra and the experimental EET rate for the LH2 system. A dielectric constant of ε_r = 2 has been used for various systems.[23,58] The largest coupling between B850 and B800 sites is then 31 cm^{-1}, the nearest-neighbor coupling in the B800 ring is 30 cm^{-1}, and the largest nearest-neighbor coupling in the B850 ring is 243 cm^{-1}.

The resulting width of the B800 peak is slightly broader than the experimental one. Making this peak narrower by reducing the magnitude of the frequency fluctuations will also lead to an increase in its height, we chose the present parameters to balance this match. We calculated the linear optical response of the LH2 complex system with the NISE[7,14] program with an average of over 1 000 000 different starting configurations with a coherence time of 384 fs.

The simulated spectrum is compared with the experimental spectrum obtained for the detergent-isolated LH2 complex from *R. acidophilus* (strain 10 050).[59] As shown in Fig. 6, the calculated absorption spectrum agrees well with the experimental one.

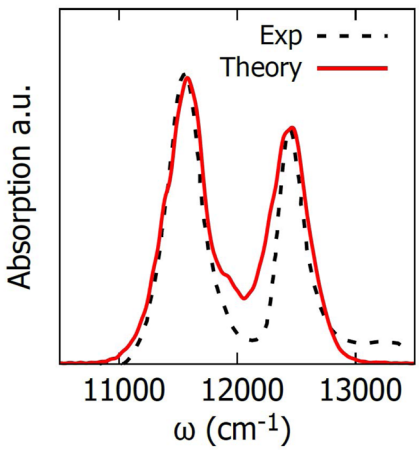

FIG. 6. Observed (black dashed line) and calculated (red solid line) absorption spectra for the LH2 system of *R. acidophilus*. Both spectra are obtained at 300 K. The measured spectrum was taken from Ref. 59.

Next, we turn to the EET rate from the B800 to the B850 ring. In Fig. 7(a), we show the transfer response obtained in the TD-MC-FRET method for this system. We see that it decays within 100 fs. Figure 7(b) gives the exponential relaxation of the total B800 population using the EET rate of 1.05 ps^{-1} obtained using our TD-MC-FRET method (black solid line). The population relaxation calculated with the NISE method (red solid line) and the population dynamics extracted from the experimental pump-probe results of the B800–B850 complex of *R. acidophilus*(blue dashed line),[48] are also shown in Fig. 7(b). The experimental rate for *Rhodoblastus acidophilus* system of 1.10 ps^{-1} has been reported.[60] The EET rate obtained from fitting the NISE population dynamics is found to be 0.79 ps^{-1}. The fit parameter c for the NISE method obtained from an average of over five independent samples was 0.968, implying a coherent component in the initial part of the transfer, explaining the difference between the NISE and TD-MC-FRET results. The calculated EET rates still have a good agreement with the experimental EET rate, which demonstrates that our developed TD-MC-FRET method is well suited to describe the EET process in the LH2 system.

Finally, we also calculated the transfer rate between two B850 units. The second unit was generated by shifting the coordinates

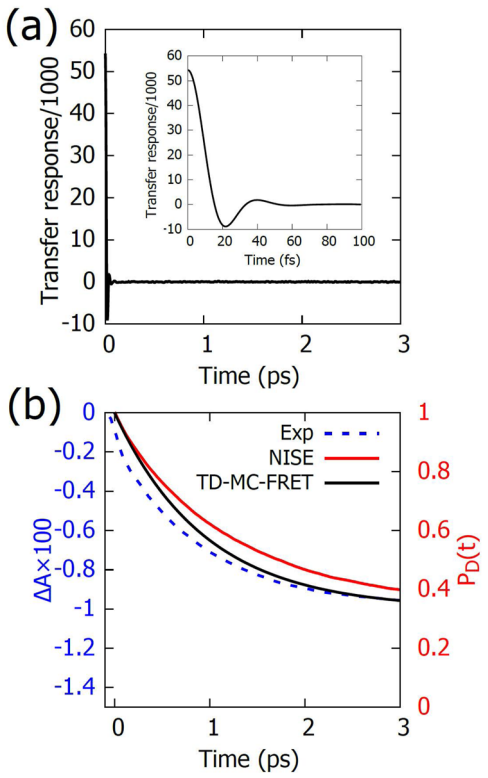

FIG. 7. (a): The B800 band to B850 band transfer response from the TD-MC-FRET method for the LH2 system. (b): The population relaxation calculated with the NISE (red solid line) and the exponential B800 population decay using the transfer rate obtained from the TD-MC-FRET method (black solid line), together with the experimental kinetics of absorbance changes in the B800–B850 complex of *Rhodoblastus acidophilus* (blue dashed line).[48]

from the pdb structure of the B850 units by 75 Å along the x-axis. We use the same parameters applied for the transfer calculation within the LH2 system. For this EET process, an experimental rate in the order of ~0.2 ps^{-1} (corresponding to a transfer lifetime of 5 ps) has been found,[61,62] while theoretically calculated EET rates in the range of 0.05–0.33 ps^{-1} (corresponding to a transfer lifetime 3–20 ps) have been reported.[63,64] Using our TD-MC-FRET and NISE methods, we obtained theoretical rates of 0.23 and 0.21 ps^{-1}, respectively. In good agreement with each other as well as with the experimental value, and in the middle of the range set by previous theoretical calculations. The *c* fit parameter for NISE, in this case, was 0.999, suggesting an entirely incoherent transfer process. The difference between the rates obtained with the two different methods, in this case, is, therefore, most likely numerical. The good agreement of the TD-MC-FRET theory results with the reference value suggests that our developed method is well suited to describe the EET transfer in the parameter regime relevant to the natural system.

IV. CONCLUSION

In this study, we developed a new version of the MC-FRET method, the TD-MC-FRET method, by combining the original version with the NISE method. The method was first demonstrated on simple model systems and subsequently applied to the LH2 complex to validate it for a realistic natural system. We found that the method is well suited for both intra- and inter-complex energy transfer.

For the system of coupled dimers, the TD-MC-FRET method was found to work very well when the dynamic disorder is large compared with the couplings. However, the TD-MC-FRET starts to fail in the small-dynamic disorder case when the transfer rate becomes larger than roughly one-tenth of the decay rate of the corresponding TD-MC-FRET transfer response. This suggests that comparing the predicted EET rate and the decay rate of the transfer response provides an initial consistency check for the TD-MC-FRET method. For the two model systems of a single donor (acceptor) surrounded by a ring of acceptors (donors), the dependence of the EET rate on the number of molecules in the ring obtained from both methods agrees very well.

Furthermore, the transfer rate for these multiacceptor (multidonor) systems can be connected by the simple relationship, $\frac{k_{x\to y}}{k_{y\to x}} = \frac{N_y}{N_x}$.

For the LH2 system, we used NISE to calculate the absorption spectrum leading to a good fit with the experimental spectrum. The B800 to B850 EET rate in LH2 was also calculated using the NISE and the TD-MC-FRET methods. Both methods gave results that compared very well to previous experimental and theoretical results. In addition, we found that the TD-MC-FRET method also describes the transfer process between two neighboring B850 rings very accurately.

Of all methods considered and compared in this work, the TD-MC-FRET method provides the most efficient way to calculate the EET rate. However, one should realize that this method is only reliable if the transfer is predominantly incoherent. As mentioned, a first consistency check can easily be performed within this method. Understanding the exciton dynamics and the excitation energy transfer for multichromophoric systems remains crucial and challenging work. For the family of TD-MC-FRET methods, this can only be solved by implementing an accurate approximation to calculate the absorption and emission responses, which in our method we achieve by using the NISE approach.

ACKNOWLEDGMENTS

H.-S.T. gratefully acknowledges the financial support from the Singapore Ministry of Education Tier 1 grant (MOE-RG14/20).

AUTHOR DECLARATIONS

Conflict of Interest

The authors have no conflicts to disclose.

Author Contributions

Kai Zhong: Formal analysis (equal); Investigation (equal); Software (equal); Visualization (equal); Writing – original draft (equal); Writing – review & editing (equal). **Hoang Long Nguyen**: Validation (supporting); Visualization (supporting); Writing – review & editing (supporting). **Thanh Nhut Do**: Validation (supporting); Visualization (supporting); Writing – review & editing (supporting). **Howe-Siang Tan**: Funding acquisition (equal); Supervision (supporting); Writing – review & editing (supporting). **Jasper Knoester**: Funding acquisition (equal); Methodology (equal); Supervision (equal); Writing – review & editing (equal). **Thomas L. C. Jansen**: Conceptualization (lead); Funding acquisition (equal); Investigation (supporting); Software (supporting); Supervision (equal); Writing – original draft (supporting); Writing – review & editing (equal).

DATA AVAILABILITY

The data that support the findings of this study are available from the corresponding author upon reasonable request.

REFERENCES

[1] T. Renger, V. May, and O. Kühn, Phys. Rep. **343**, 137 (2001).
[2] H.-Q. Peng, L.-Y. Niu, Y.-Z. Chen, L.-Z. Wu, C.-H. Tung, and Q.-Z. Yang, Chem. Rev. **115**, 7502 (2015).
[3] P. Huo and D. F. Coker, J. Chem. Phys. **133**, 184108 (2010).
[4] S. Caffarri, K. Broess, R. Croce, and H. van Amerongen, Biophys. J. **100**, 2094 (2011).
[5] S. Jang, M. D. Newton, and R. J. Silbey, Phys. Rev. Lett. **92**, 218301 (2004).
[6] S. Jang, M. D. Newton, and R. J. Silbey, J. Phys. Chem. B **111**, 6807 (2007).
[7] T. l. C. Jansen and J. Knoester, J. Phys. Chem. B **110**, 22910 (2006).
[8] O. Sinanoğlu, *Modern Quantum Chemistry: Action of Light and Organic Crystals* (Academic Press, 1965).
[9] H. Haug, V. M. Agranovich, and M. D. Galanin, *Electronic Excitation Energy Transfer in Condensed Matter* (North-Holland, Amsterdam, 1983).
[10] K. Mukai, S. Abe, and H. Sumi, J. Phys. Chem. B **103**, 6096 (1999).
[11] J. Ma and J. Cao, J. Chem. Phys. **142**, 094106 (2015).
[12] V. M. Kenkre and P. Reineker, *Exciton Dynamics in Molecular Crystals and Aggregates*, Springer tracts in modern physics (Springer Berlin Heidelberg, Berlin, Heidelberg, 1982), Vol. 94.
[13] T. Kunsel, T. L. C. Jansen, and J. Knoester, J. Chem. Phys. **155**, 134305 (2021).
[14] C. Liang and T. L. C. Jansen, J. Chem. Theory Comput. **8**, 1706 (2012).
[15] T. l. C. Jansen and J. Knoester, Acc. Chem. Res. **42**, 1405 (2009).
[16] A. S. Bondarenko, J. Knoester, and T. L. C. Jansen, Chem. Phys. **529**, 110478 (2020).
[17] Y. Tanimura and R. Kubo, J. Phys. Soc. Jpn. **58**, 101 (1989).

[18] A. Ishizaki and G. R. Fleming, J. Chem. Phys. **130**, 234110 (2009).
[19] J. Strümpfer and K. Schulten, J. Chem. Theory Comput. **8**, 2808 (2012).
[20] C. P. van der Vegte, A. G. Dijkstra, J. Knoester, and T. L. C. Jansen, J. Phys. Chem. A **117**, 5970 (2013).
[21] H. Sumi, J. Phys. Chem. B **103**, 252 (1999).
[22] D. L. Andrews and A. A. Demidov, *Resonance Energy Transfer* (Wiley, 1999).
[23] C.-P. Hsu, G. R. Fleming, M. Head-Gordon, and T. Head-Gordon, J. Chem. Phys. **114**, 3065 (2001).
[24] A. S. Davydov, Sov. Phys. Usp. **7**, 145 (1964).
[25] V. May and O. Kühn, *Charge and Energy Transfer Dynamics in Molecular Systems* (John Wiley & Sons, 2008).
[26] V. Czikkely, H. D. Försterling, and H. Kuhn, Chem. Phys. Lett. **6**, 11 (1970).
[27] C. Didraga, A. Pugžlys, P. R. Hania, H. von Berlepsch, K. Duppen, and J. Knoester, J. Phys. Chem. B **108**, 14976 (2004).
[28] M. E. Madjet, A. Abdurahman, and T. Renger, J. Phys. Chem. B **110**, 17268 (2006).
[29] T. Renger, Photosynth. Res. **102**, 471 (2009).
[30] C. P. van der Vegte, J. D. Prajapati, U. Kleinekathöfer, J. Knoester, and T. L. C. Jansen, J. Phys. Chem. B **119**, 1302 (2015).
[31] S. M. Prince, M. Z. Papiz, A. A. Freer, G. McDermott, A. M. Hawthornthwaite-Lawless, R. J. Cogdell, and N. W. Isaacs, J. Mol. Biol. **268**, 412 (1997).
[32] D. Cringus, T. l. C. Jansen, M. S. Pshenichnikov, and D. A. Wiersma, J. Chem. Phys. **127**, 084507 (2007).
[33] T. Förster, Ann. Phys. **437**, 55 (1948).
[34] V. Novoderezhkin, A. Marin, and R. van Grondelle, Phys. Chem. Chem. Phys. **13**, 17093 (2011).
[35] A. S. Sardjan, F. P. Westerman, J. P. Ogilvie, and T. L. C. Jansen, J. Phys. Chem. B **124**, 9420 (2020).
[36] S. Mukamel, *Principles of Nonlinear Optical Spectroscopy* (Oxford University Press on Demand, 1999), Vol. 6.
[37] S. Jang and R. J. Silbey, J. Chem. Phys. **118**, 9324 (2003).
[38] K. Mukai, S. Abe, and H. Sumi, J. Lumin **87**, 818–820 (2000).
[39] M. Aghtar, J. Liebers, J. Strümpfer, K. Schulten, and U. Kleinekathöfer, J. Chem. Phys. **136**, 214101 (2012).
[40] T. L. C. Jansen, J. Phys. Chem. A **122**, 172 (2018).
[41] A. Bastida, C. Cruz, J. Zúñiga, A. Requena, and B. Miguel, Chem. Phys. Lett. **417**, 53 (2006).
[42] D. W. Oxtoby, Annu. Rev. Phys. Chem. **32**, 77 (1981).
[43] T. Kunsel, V. Tiwari, Y. A. Matutes, A. T. Gardiner, R. J. Cogdell, J. P. Ogilvie, and T. L. C. Jansen, J. Phys. Chem. B **123**, 394 (2019).
[44] W. Kleinekofort, L. Germeroth, J. A. van den Broek, D. Schubert, and H. Michel, Biochim. Biophys. Acta, Bioenerg. **1140**, 102 (1992).
[45] M. Z. Papiz, S. M. Prince, T. Howard, R. J. Cogdell, and N. W. Isaacs, J. Mol. Biol. **326**, 1523 (2003).
[46] T. Pullerits and V. Sundström, Acc. Chem. Res. **29**, 381 (1996).
[47] N. Hartigan, H. A. Tharia, F. Sweeney, A. M. Lawless, and M. Z. Papiz, Biophys. J. **82**, 963 (2002).
[48] J. T. M. Kennis, A. M. Streltsov, S. I. E. Vulto, T. J. Aartsma, T. Nozawa, and J. Amesz, J. Phys. Chem. B **101**, 7827 (1997).
[49] O. Rancova, J. Sulskus, and D. Abramavicius, J. Phys. Chem. B **116**, 7803 (2012).
[50] G. D. Scholes and G. R. Fleming, J. Phys. Chem. B **104**, 1854 (2000).
[51] L. Cleary and J. Cao, New J. Phys. **15**, 125030 (2013).
[52] A. Ishizaki and G. R. Fleming, Proc. Natl. Acad. Sci. **106**, 17255–17260 (2009).
[53] J. Strümpfer and K. Schulten, J. Chem, Phys. **131**, 225101 (2009).
[54] M. H. C. Koolhaas, R. N. Frese, G. J. S. Fowler, T. S. Bibby, S. Georgakopoulou, G. van der Zwan, C. N. Hunter, and R. van Grondelle, Biochem **37**, 4693 (1998).
[55] T. H. P. Brotosudarmo, A. M. Collins, A. Gall, A. W. Roszak, A. T. Gardiner, R. E. Blankenship, and R. J. Cogdell, Biochem **440**, 51 (2011).
[56] L. Cleary, H. Chen, C. Chuang, R. J. Silbey, and J. Cao, Proc. Natl. Acad. Sci. U. S. A. **110**, 8537 (2013).
[57] W. Humphrey, A. Dalke, and K. Schulten, J. Mol. Graphics **14**, 33 (1996).
[58] T. Renger and F. Müh, Photosynth. Res. **111**, 47 (2012).
[59] Y.-Z. Ma, R. J. Cogdell, and T. Gillbro, J. Phys. Chem. B **101**, 1087 (1997).
[60] V. Moulisová, L. Luer, S. Hoseinkhani, T. H. P. Brotosudarmo, A. M. Collins, G. Lanzani, R. E. Blankenship, and R. J. Cogdell, Biophys. J. **97**, 3019 (2009).
[61] R. Agarwal, A. H. Rizvi, B. S. Prall, J. D. Olsen, C. N. Hunter, and G. R. Fleming, J. Phys. Chem. A **106**, 7573 (2002).
[62] M. Escalante, A. Lenferink, Y. Zhao, N. Tas, J. Huskens, C. N. Hunter, V. Subramaniam, and C. Otto, Nano Lett. **10**, 1450 (2010).
[63] D. E. Chandler, J. Strümpfer, M. Sener, S. Scheuring, and K. Schulten, Biophys. J. **106**, 2503 (2014).
[64] S. Jang, E. Rivera, and D. Montemayor, J. Phys. Chem. Lett. **6**, 928 (2015).